CHALMERS
UNIVERSITY OF TECHNOLOGY

Impact of Environmental Factors on Breakdown Characteristics of Air Insulation in Power Distribution Components of Electrical Aircraft

Master's Thesis in
Sustainable Electric Power Engineering and Electromobility Program

ALI KOSEOGLU

DEPARTMENT OF ELECTRICAL ENGINEERING

CHALMERS UNIVERSITY OF TECHNOLOGY
Gothenburg, Sweden, 2025
www.chalmers.se

MASTER'S THESIS 2025

Impact of Environmental Factors on Breakdown Characteristics of Air Insulation in Power Distribution Components of Electrical Aircraft

ALI KOSEOGLU

CHALMERS
UNIVERSITY OF TECHNOLOGY

Department of Electrical Engineering
CHALMERS UNIVERSITY OF TECHNOLOGY
Gothenburg, Sweden 2025

Impact of Environmental Factors on Breakdown Characteristics of Air Insulation in Power Distribution Components of Electrical Aircraft
Ali Koseoglu

Supervisor: Yuriy Serdyuk, Chalmers University of Technology Department of Electrical Engineering
Supervisor: Naveen Raja Rajarathinam, Heart Aerospace
Examiner: Yuriy Serdyuk, Chalmers University of Technology Department of Electrical Engineering

Master's Thesis 2025
Department of Electrical Engineering
Chalmers University of Technology
SE-412 96 Gothenburg Sweden
Telephone: +46 31 772 1000

Cover:
Heart ES-30™ electric aircraft illustration, courtesy of Heart Aerospace AB, 2025.

Gothenburg, Sweden 2025

Impact of Environmental Factors on Breakdown Characteristics of Air Insulation in Power Distribution Components of Electrical Aircraft

ALI KOSEOGLU
Department of Electrical Engineering
Chalmers University of Technology

Abstract

Growing concerns on environmental issues challenge scientists and engineers to create greener technologies on a vast area of industrial and commercial applications. Aviation, as one of the major human activities responsible for the environmental impacts, is among the most trending topics in this effort for transition to more eco-friendly technologies.

While electrical aircraft have been experimented from as early as 1885, achieved by Gaston Tissandier by flying a small airship powered by an electric motor, the scale of aircraft needed today is significantly larger. The more powerful electrical powertrains needed to achieve this goal call for higher levels of system voltage to reduce the weight and enable competitive designs.

Although well-studied for land and sea applications, the use of high voltage systems is a relatively new area for aviation systems. A growing demand for research and development is emerging for creating regulations, technical standards, testing methods and know-how for applying high voltage solutions in electrical aircraft.

This thesis explored the implications of implementing high voltage direct current systems to be used in hybrid or all-electric electrical aircraft with a focus on the performance of the dielectric systems under expected ambient conditions in high altitudes, namely extreme ambient temperatures (T_A), low air pressure (p) and various relative humidity (RH) levels.

To achieve the goal, experimental setups of vacuum and climate conditioning chambers were utilized to create ambient conditions an electrical aircraft may experience, and respective breakdown voltage for the insulation system for various scenarios were measured.

It was observed that lower air pressure and relative humidity levels create unfavorable conditions for the insulation system, while lower ambient temperature increases the breakdown voltage. The combined effect of higher altitude conditions was evaluated to be of performance depreciative nature for the insulation systems as the altitude increases up to 25,000 feet. It was also concluded that significantly lower insulation performance may emerge around the dew point of water in the air.

Keywords: High Voltage Direct Current, Electric Aircraft, Insulation Systems, Townsend Mechanism, Paschen's Law, Non-Uniform Electrical Fields, Breakdown Test, Vacuum Chamber, Climate Chamber.

Acknowledgements

I would like to start by thanking my supervisors Prof. Yuriy Serdyuk, Chalmers University of Technology, and Dr. Naveen Raja Rajarathinam, Heart Aerospace, for their valuable feedback and insightful discussions.

I would also like to thank Doc. Thomas Hammarström and Daniel Svensson from Chalmers University of Technology Department of Electrical Engineering for their support in configuring the measurement systems.

Last but not less importantly, Herold Fuentes Diaz also deserves my thanks for his collaboration in photography.

Ali Koseoglu, Gothenburg, 2025-02-21

List of Abbreviations

d	Gap length / distance between electrodes (m)
E	Electrical field strength (V/m)
E_0	Mean electrical field strength (V/m)
E_i	Critical electrical field strength (V/m)
E_{max}	Maximum electrical field strength (V/m)
IPCC	Intergovernmental Panel on Climate Change
NOAA	National Oceanic and Atmospheric Administration
p	Gas pressure (bar)
RH	Relative humidity (%)
T_A	Ambient temperature (K or °C)
U_{bd}	Breakdown voltage (V)
$U_{bd\ min}$	Minimum breakdown voltage (V)
ε_r	Relative permittivity
η	Field efficiency factor or utilization factor

Table of Contents

List of Figures

List of Tables

1

Introduction

Environmental issues are defined as the set of challenges and problems facing Earth and its natural systems. These issues are usually complex and interconnected and comprises a wide range of topics from climate change and pollution to overpopulation and energy use. The environmental issues have impact on health of the natural world, but in no small part, have negative impacts on human health and well-being, organizations, and business operations. [1]

It is known that environmental issues arise both from natural causes and human activities. The Earth's ecosystems have the capability to manage certain amounts of natural disturbances like forest fires and floods, but human activities can create circumstances in which the disturbances happen with greater frequency or intensity. [1]

While environmental concerns cover a vast area of aspects like biodiversity loss, deforestation, plastic pollution, ocean acidification, melting ice caps and sea level rise; global warming from fossil fuels is arguably the most alarming one of the topics. [2]

The year 2023 has been registered as the warmest year since global temperature recordings were initiated in 1850. The global average temperature was measured as 1.18 °C (2.12 °F) above the 20^{th} Century average of 13.9 °C (57.0 °F), which is 0.15 °C (0.27 °F) higher than the previous record set in 2016. It must also be noted that the 10 warmest years since 1850 have all been recorded during the last decade (2014–2023). [3]

In addition to record-high global average temperature, it has been found out that carbon dioxide (CO_2) level in the atmosphere is also setting records. CO_2 level in the atmosphere is known to be stable around 280 parts per million (ppm) for almost 6,000 years of human civilization, now is measured to be well above 420 ppm, significantly higher than what it was the onset of the Industrial Revolution in the 19^{th} century. National Oceanic and Atmospheric Administration (NOAA) Administrator Rick Spinrad interprets the steady annual increase in atmospheric CO_2 as a direct result of human activity, and states that the main contribution sources are burning of

fossil fuels for transportation, electricity generation, cement manufacturing, deforestation, and agricultural activities. [2]

The Intergovernmental Panel on Climate Change (IPCC), the United Nations body for assessing the science related to climate change, evaluates that the climate change is a threat both for human well-being and planetary health and any delays in global efforts on adaptation and mitigation will miss a brief and rapidly closing window of opportunity to secure a livable and sustainable future for all. [4]

Aviation is one of the major human activities responsible for the environmental impacts. Aviation has been growing considerably in the recent decades, and it is known that aviation activities accounts for approximately 2 percent of global carbon dioxide emissions, well-known to be a greenhouse gas, and some 4 percent of all climate change impacts annually, as well as other negative environmental impacts like particulate matter formation from particle emissions, acidic emissions (e.g., nitrogen oxides) and ground-level ozone formation from emissions of nitrogen oxides and hydrocarbons. [5]

The European Green Deal, approved in 2020 by the European Commission is a set of policy initiatives to achieve climate neutrality by 2050, aims to reduce transport emissions by 90% compared to 1990-levels by 2050. The aviation sector, creating 13.9% of the carbon dioxide emissions from transport as of 2017, will be an important part of the effort [6], therefore, there is a clear incentive for cleaner, greener air mobility.

While aviation is an important contributor to climate change and other environmental problems, electrification is one option for reducing these environmental impacts [5]. Electrical propulsion systems help the reduction of CO_2, nitrogen oxides (NO_X), fine particulate matter and ozone (O_3) emissions, as well as reducing noise and fuel consumption. In terms of fuel efficiency and emissions reduction for aircraft, it is observed that technical improvements in jet engines have reached a plateau (see Figure 1) [7]. There is an opportunity to potentially reduce harmful emissions meaningfully further and to make air travel quieter for urban area by introducing electric battery-powered aircrafts [7].

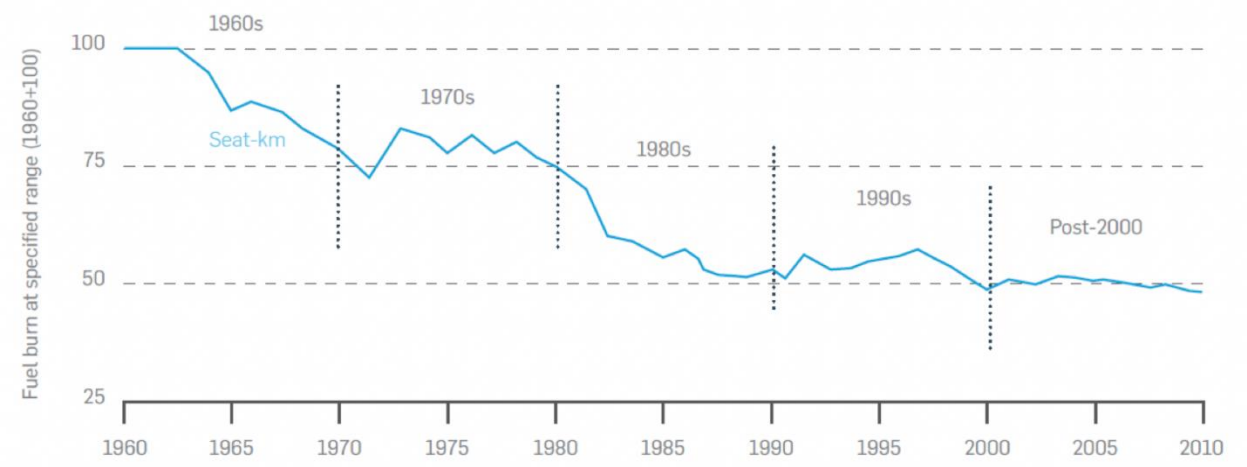

Figure 1: Average fuel burn for new jet aircraft

There are many technical challenges to implement electrical propulsion into aircrafts, and most of the challenges arise from the need of reducing weight, e.g., overcoming the low energy density of batteries today's technology offers [8], and the need for more efficient and lighter electrical motors [9].

One of the methods to reduce electrical systems' weight that is needed for electrical propulsion is to increase the battery pack and the respective direct current (DC) system voltage to decrease electrical current flow needed while achieving the same power transfer between the energy storage system and electrical motors, therefore reducing power cabling weight.

However, usage of higher voltages in aircraft is relatively new, and technical standards, regulations and studies on the area are scarce.

1.1.Aim

The aim of this project is to explore the possible implications of implementing high voltage direct current systems to be used in hybrid or all-electric electrical aircraft with a focus on the performance of the dielectric systems under expected ambient conditions in high altitudes, namely extreme ambient temperatures, low air pressure (p) and various relative humidity (RH) levels. The output will be evaluated to discuss and conclude the changes in electrical insulation systems' performance at relevant ambient conditions that electrical aircraft is likely to experience.

1.2. Objectives

More specifically, the following tasks will be considered:

- What are the underlying mechanisms that defines the performance of insulation systems for electric aircraft?
- How does the air pressure influence the breakdown voltage of insulation systems?
- How does the ambient temperature influence the breakdown voltage of insulation systems?
- What is the effect of relative humidity of air on breakdown voltage of insulation systems?
- Are there any critical conditions in terms of ambient conditions that may have a significant effect on breakdown voltage?

1.3. Limitations

The study will be limited to exploring the high-altitude ambient parameters of air pressure, ambient temperature, and relative humidity. Other parameters that may influence the insulating systems such as the amount of atmospheric free charges and chemical composition of the atmosphere will not be in the scope of this work.

2

Background and Theory

Aircraft development programs are continuously challenged on minimization of weight, reduction of aircraft drag and rate of engine fuel burn. Achieving an aircraft design with lowest feasible weight is crucial for competitiveness in unit and maintenance costs. [10]

Figure 2 gives an overview of important technical voltage stresses in high voltage engineering. [11]

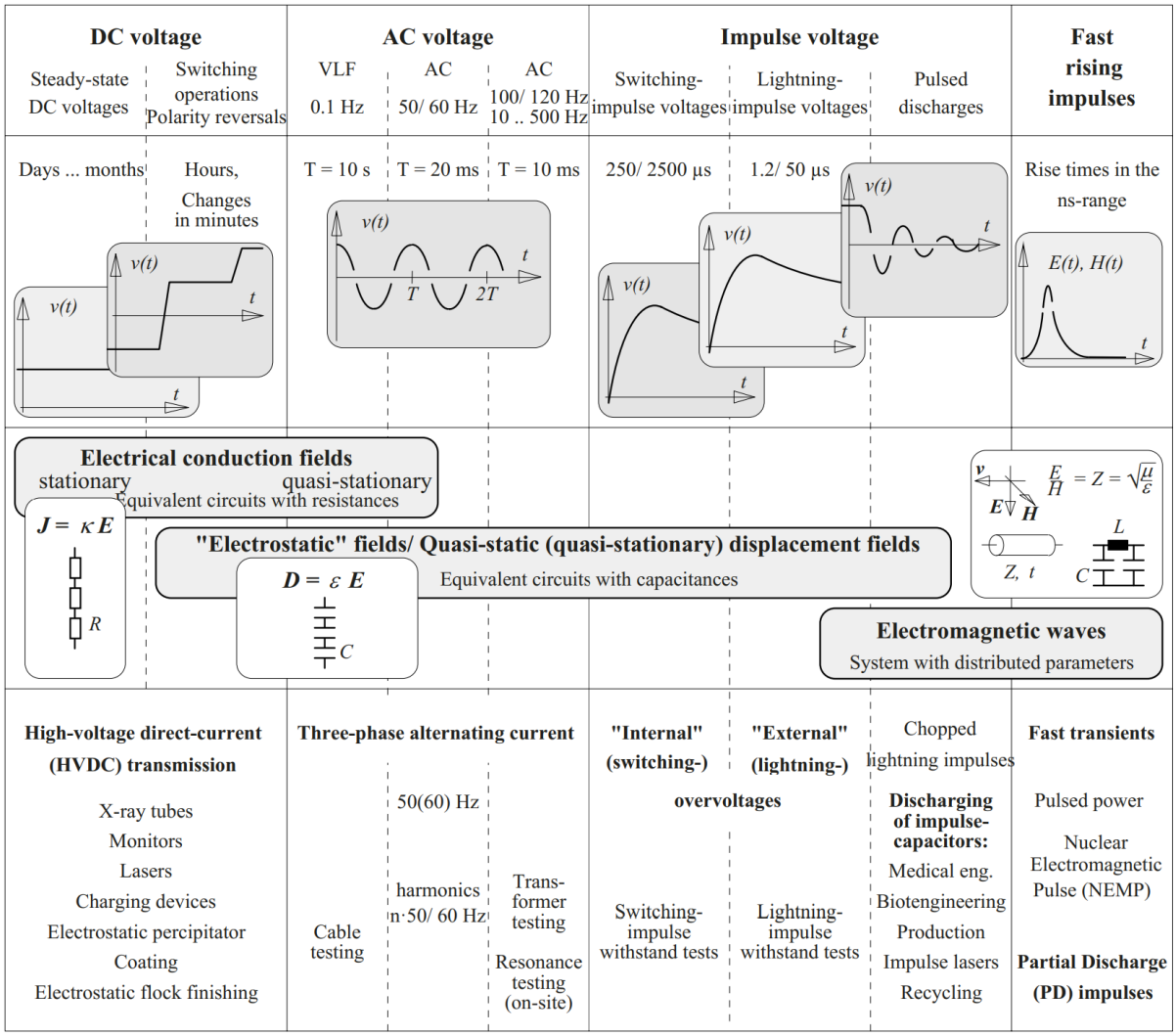

Figure 2: Overview of important technical voltage stresses in high voltage engineering

2.1. Gases and Ambient Air as Insulation Mediums

Gases, included ambient air, are considered natural insulating materials having low electrical power losses, high electrical resistance values and low relative permittivity ($\varepsilon_r \approx 1$) almost independently from voltage frequency [11]. Additionally, the fact that air insulation adds no extra weight to aircraft weight is of particularly high value for aircraft design. Therefore, ambient air is the medium of choice for aircraft for most cases, and liquid or solid insulating materials are avoided as much as possible where the electric strength of the air is sufficient.

Another technical advantage of using gases and ambient air is that the physical properties of gases are very well defined and breakdown voltage level for a given homogenous electrical field can be modelled mathematically [11], making modelling and predictions easier.

On the other hand, most gases, including ambient air, are known to have a significantly lower electric strength compared to solids and liquids, and where characteristic electrical stress conditions lead to gas discharges and electrical breakdown at usually lower voltage values compared to liquid and solid dielectrics. [11]

Electrical discharges are defined as the release and transmission of electricity in an applied electric field through a medium [12]. Gases, like every other form of insulating mediums, experience discharges under electric field stress that is greater than zero. Ohm's Law gives the current as

$$I = \frac{V}{R} \qquad (1)$$

where I is the current in Amperes, V is the applied voltage in Volts and R is the resistance in Ohms. As the resistance always have a finite value in practice, there is always a current flowing in a circuit where a voltage bigger than zero is applied.

It must be noted that discharges are sub-categorized according to the physical mechanism involved in the discharge event and not all discharges are breakdowns; pre-discharges are typically relatively small current discharges that do not cause a direct collapse of the resistance between electrodes, while breakdowns or flashovers are electrical discharges cause a very conductive channel between electrodes. [11]

The following section explores the different mechanisms involved in the pre-discharge and breakdown phenomena in dielectric gases.

2.1.1. Mechanism of Breakdown in Gases under Uniform Electrical Fields

2.1.1.1. Townsend Mechanism

The Townsend mechanism describes the process of electrical breakdown in gases, which occurs when a gas becomes ionized and conducts electricity.

The ionization process develops when free electrons are accelerated by an electric field, collide with gas molecules, and consequently free additional electrons, which are in turn accelerated and free even more additional electrons. The process results in an avalanche multiplication that permits significantly increased electrical conduction through the gas. [13]

The key points of the Townsend mechanism are as follows:

- Ionization by Collision: Naturally occurring free electrons gain energy from an electric field and collide with gas molecules, ionizing them and creating more free electrons and positive ions.
- Avalanche Effect: The newly created electrons are accelerated by the electric field, leading to further collisions and ionization. This creates an avalanche of electrons, rapidly increasing the number of charged particles.

- Critical Conditions: For breakdown to occur, the number of ionized particles must reach a critical level. This is influenced by factors such as the electric field strength, gas pressure, and the type of gas.
- Paschen's Law: The Townsend mechanism is often described in the context of Paschen's Law, which relates the breakdown voltage to the product of gas pressure and electrode distance.

2.1.1.2. Paschen's Law

Louis Carl Heinrich Friedrich Paschen (22 January 1865 - 25 February 1947), a German physicist, made extensive studies on electrical breakdown voltage of various gases with a symmetrical experimental setup of parallel metal plates with various gas pressure and gap distance configurations. He derived a mathematical equation to fit the experimental result curves, which was later coined as *Paschen's Law* [14].

While Paschen's Law gives the mathematical solution only for uniform electric fields, which hardly exists in industrial designs and applications, it provides fundamental information for understanding on the behavior of dielectric gases under electrical stress and related breakdown mechanisms with regards to influence of gas pressure and interelectrode gap length.

Paschen's Law suggests that,

A. When the gap between electrodes (d) is kept constant, after a critical inter-electrode gas pressure is reached, the breakdown voltage increases as the pressure increases. A pressure below that critical value produces the opposite inclination, where the breakdown voltage increases with decreasing pressure,
B. When the insulation gas pressure (p) is kept constant, after a critical gap distance is reached, the breakdown voltage increases as the gap between electrodes increases. A gap distance below that critical value produces the opposite inclination, where the breakdown voltage increases with decreasing gap distance.

The critical value of gap by pressure product ($(p \cdot d)_{min}$ in Figure 3) is gives the minimum breakdown voltage ($U_{bd\,min}$) and it indicates that there exists a minimum sparking potential for an electrode configuration [15], below which a breakdown cannot occur. [11]

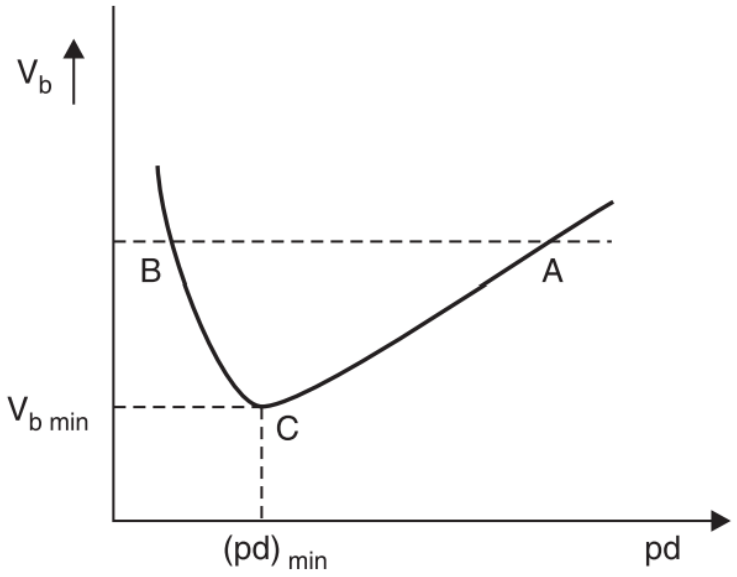

Figure 3: A Representation of Paschen's Curve

The characteristics of the Paschen curve varies by the insulating gas; critical value of $p \cdot d$ and the $U_{bd\ min}$ differs for each gas (Figure 4). [16]

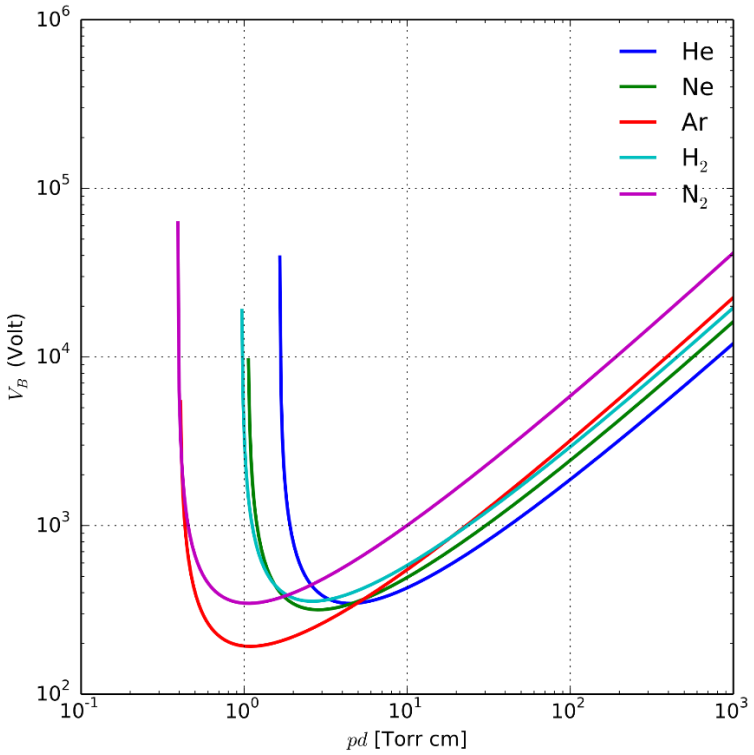

Figure 4: Paschen's curve for various gases

Table 1 gives experimentally obtained minimum breakdown voltage values for various gases [11]. The table clearly shows that specific breakdown voltage for different gases vary in a wide range.

Table 1: Paschen minima for different gases

Gas	$V_{bd\ min}$/ V	$(pd)_{min}$/ bar·µm
SF_6	507	3.5
O_2	450	9.3
CO_2	420	6.8
Air	330 350	7.3
N_2	240 250	8.6
H_2	230 270	14
Ne	129 245	53.2
Ar	94 265	-
He	155	53.2

2.1.2. Mechanism of Breakdown in Gases under Non-uniform Electrical Fields

Non-uniform electrical fields are defined as electrical field distributions where the maximum field strength E_{max} in the field differs from the mean field strength between the electrodes. The ratio between these field values is defined as *field efficiency factor* or *utilization factor* and is calculated as

$$\eta = \frac{E_o}{E_{max}} \qquad (2)$$

where η stands for field efficiency factor ($1 \geq \eta > 0$), E_0 (V/m) for mean field strength and E_{max} (V/m) for maximum field strength. [11]

With a homogeneous insulating gas between electrodes (e.g., air), field efficiency factor merely depends on the shapes of the electrodes and the distance between them.

The breakdown voltage is strongly influenced by the field efficiency factor and is inversely proportionate to η, thus, lower breakdown voltage levels emerge as the field distribution is distorted.

The calculation or estimation of breakdown voltage methods for different ranges of field efficiency factor is given below.

- For very weakly non-uniform electric fields where $1 > \eta \geq 0.8$, the breakdown voltage is calculated as for uniform fields and are valid for direct current and alternating voltage as well as impulse voltages like switching and lightning.

- For weakly non-uniform electric fields where $0.8 > \eta > 0.2$, the breakdown voltage is calculated as

$$U_{bd} = E_i \cdot \eta \cdot d \qquad (3)$$

  where U_{bd} stands for breakdown voltage (V), E_i for critical electric field strength (V/m), η for field efficiency factor and d (m) for distance between the electrodes.

- For strongly non-uniform electric fields where $0.2 \geq \eta > 0$, where (unlike for weaker field efficiency factors) pre-discharges occur before the breakdown is reached, and the breakdown voltage is not precisely calculable, but there are mathematical methods that enable rough estimations. [11]

Industrial electrical components are designed to have field efficiency factors as close as possible to 1, to enhance electrical withstand levels, however, it is not always possible to achieve very high η levels due to functionality requirements (such as reducing product size and limitations on physical arrangement of components), cost reducing concerns and unavoidable physical phenomena (e.g. thermal gradients in the insulating medium).

The electrical components in the electrical aircraft are no exception. In this study, an essential electrical component, a fuse holder in combination with a ceramic fuse link, which has one of the most strongly non-uniform electrical field distribution among the other components, was experimented to explore breakdown voltage levels under various ambient conditions.

3

Methods

3.1. The Test Object

A DC power distribution box configuration with a rated system voltage of 800 V_{DC} was selected as a test object, comprising a metal enclosure with metal mounting plate, a 160 A rated fuse base[1] (Figure 5) and a melting element type ceramic fuse[2] (Figure 6) with 125 A rated current. The fuse holder combined with the fuse was mounted in the metal enclosure (Figure 7). The distribution box rating was evaluated through the consideration of the insulating element's rated insulation voltage, which is the fuse base for the test object.

[1] Eaton Bussmann SD00-D series fuse base. Product specifications available at https://www.eaton.com/gb/en-gb/skuPage.SD00-D.pdf

[2] Eaton Bussmann series 125NHG00B fuse. Product specifications available at https://www.eaton.com/gb/en-gb/skuPage.125NHG00B.pdf

Figure 5: 160 A rated fuse base

Figure 6: 125 A rated ceramic fuse

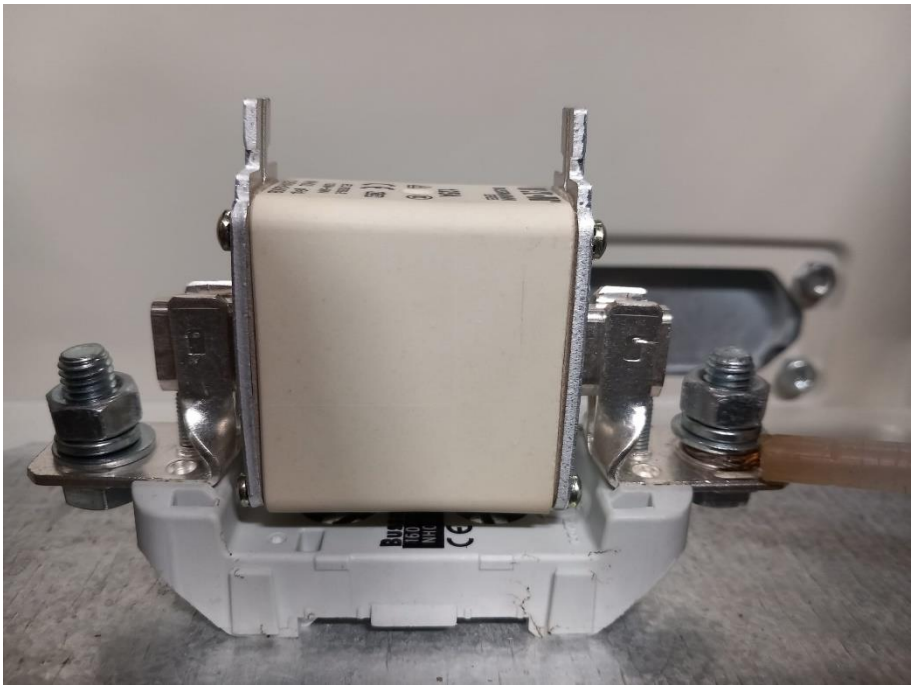

Figure 7: Fuse holder combined with fuse link

3.2. Vacuum Chamber Setup

The test setup for evaluation of air pressure influence on breakdown voltage levels, which will be called as *Vacuum Chamber Setup* from here on, comprised a custom-made vacuum chamber equipped with a vacuum pump (Pfeiffer Pascal 2015SD [3]), a direct current voltage source (Glassman Series FJ [4]), a resistive voltage divider for DC voltage measurements (Cal Test CT4028 [5]), a shunt resistor as the current sensor, an oscilloscope for monitoring and capturing the data (Tektronix TDS2004B [6]) and a PC to record the oscilloscope output. The setup schema is given in Figure 8 and the setup photo in Figure 9.

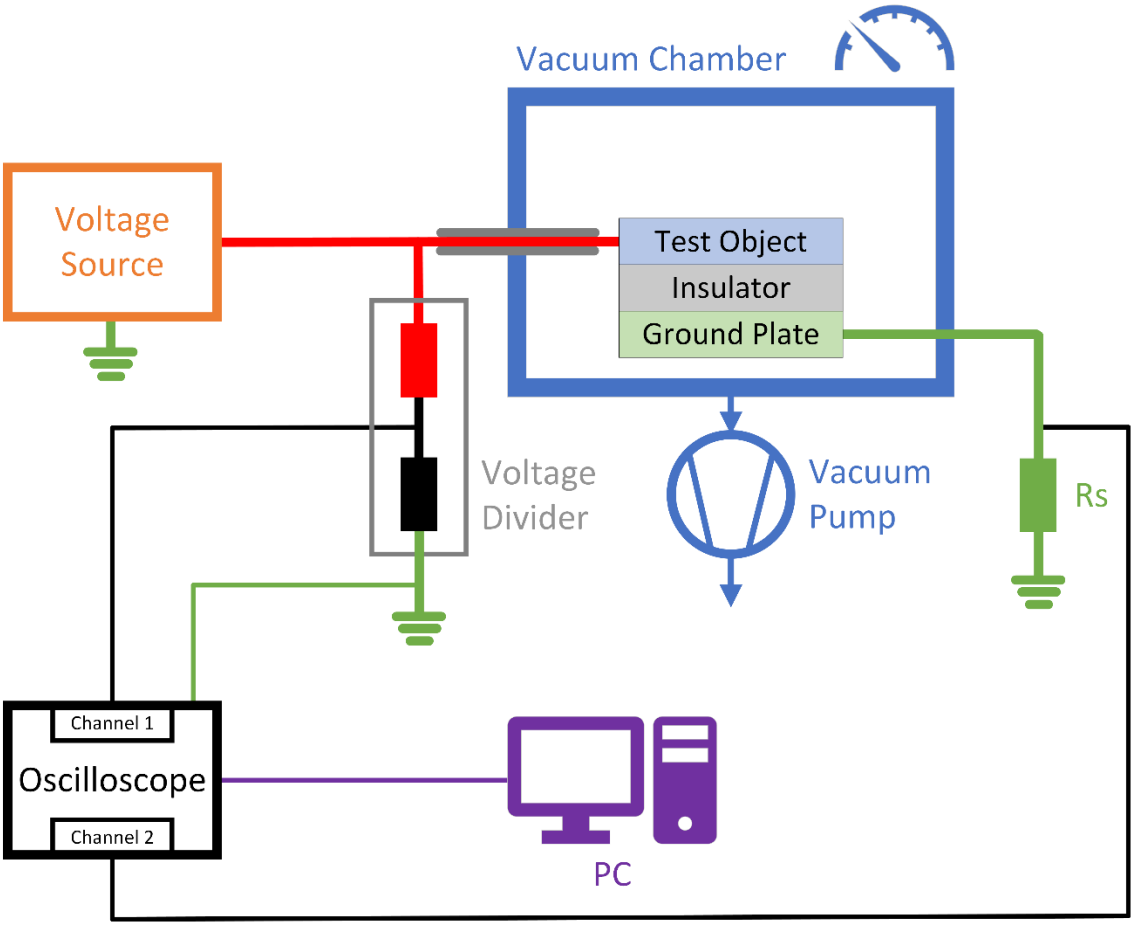

Figure 8: The vacuum chamber setup schema

[3] Technical characteristics available on https://cdn.abicart.com/shop/ws28/75628/art72/156026972-f43393-215SDMHEM.en.pdf
[4] Datasheet available on: https://www.amstechnologies-webshop.com/media/pdf/00/58/f0/FJ-Series-High-Voltage-AC_DC-Power-Supplies-XP-Glassman-Datasheet.pdf
[5] Datasheet available on: https://www.farnell.com/datasheets/2580814.pdf
[6] Datasheet available on: https://www.testequipmenthq.com/datasheets/TEKTRONIX-TDS2004B-Datasheet.pdf

Figure 9: The vacuum chamber photograph

3.3. Climate Chamber Setup

The test setup for evaluation of ambient temperature and humidity influence on breakdown voltage levels, which will be called as *Climate Chamber Setup* from here on, comprised a climate chamber with temperature and humidity control (Weisstechnik ClimeECO C7-340 [7]), a direct current voltage source (Glassman Series FJ), a resistive voltage divider for DC voltage measurements (Cal Test CT4028), a shunt resistor as the current sensor, an oscilloscope for monitoring and capturing the data (Tektronix TDS2004B) and a PC to record the oscilloscope output. The setup schema is given in Figure 10 and the setup photo in Figure 11.

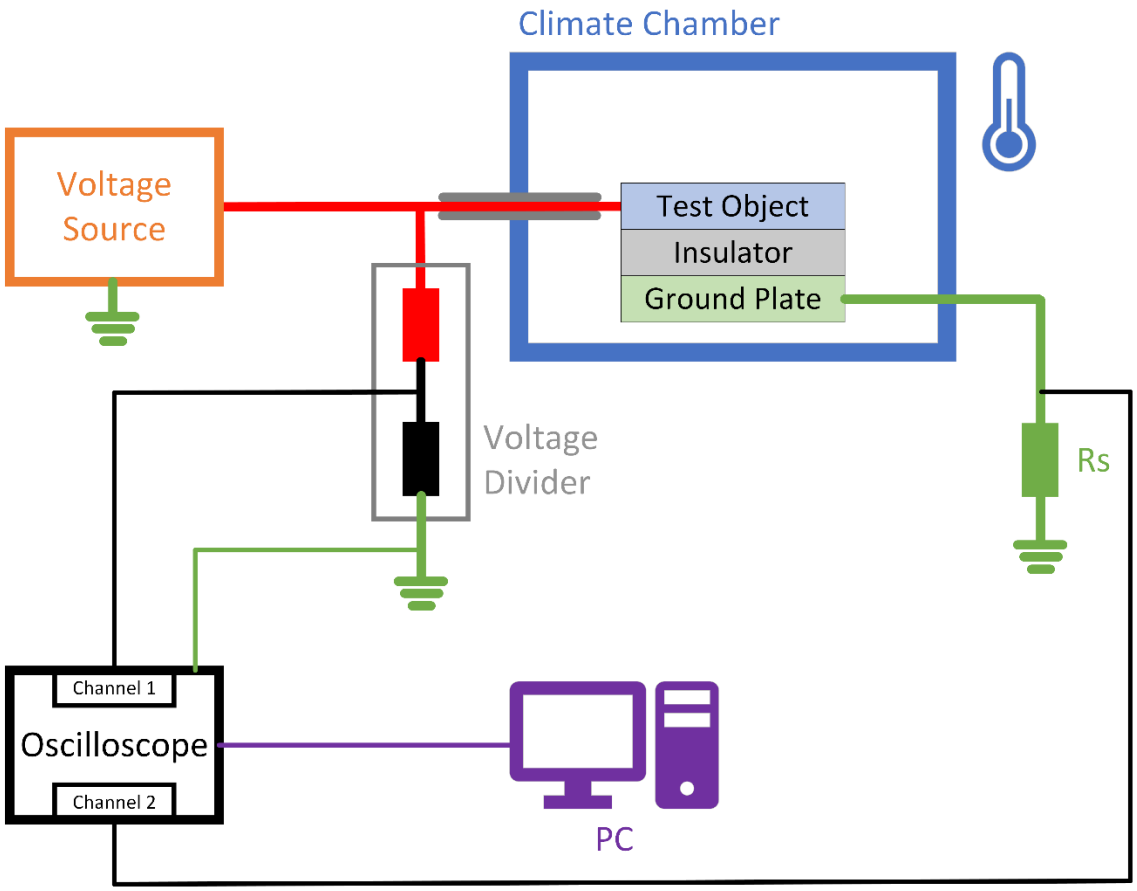

Figure 10: The climate chamber setup schema

[7] Technical characteristics and product information available on: https://www.weiss-technik.com/environmental-simulation/en/detailpages/climeeco

Figure 11: The climate chamber setup photograph

It must be noted that certain combinations of air pressure and temperature results in critical state for water in the air, namely the *phase transition*. See Figure 12 for the phase diagram of water [17].

For the reason mentioned above, the phase of water in the air cannot be estimated and set precisely around 0 °C at sea-level atmospheric pressure and normal temperature conditions, which leads to uncertainty in predicting the performance of air insulation, as the intrinsic insulating properties of solid, liquid and gaseous phases of water are remarkably different.

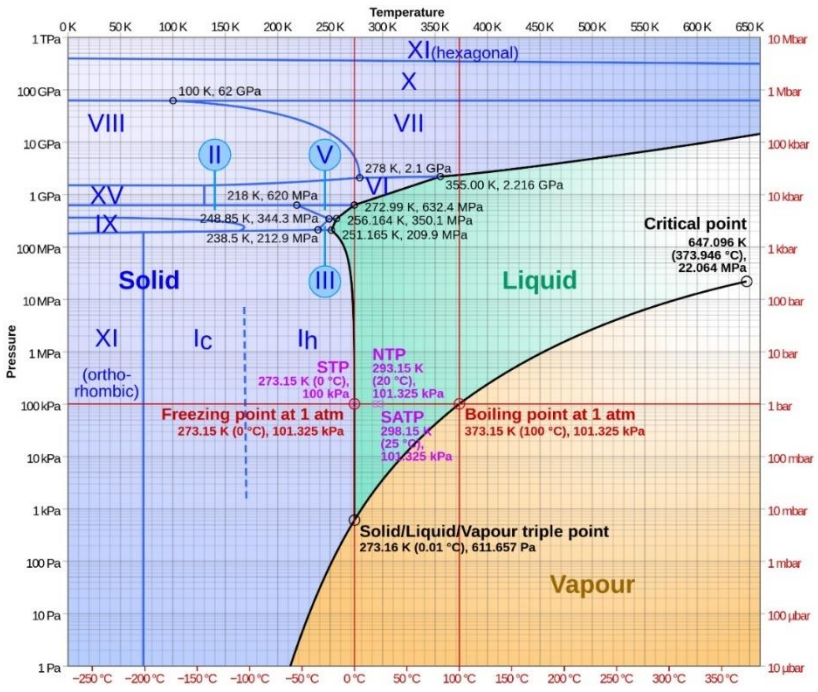

Figure 12: Phase diagram of water including high-pressure forms ice II, ice III, etc.

The capabilities of the climate chamber in terms of setting the humidity in certain thermal conditions are limited due to the phenomena around the phase transition boundaries of water mentioned above. Figure 13 [18] shows the available configuration range of the climate chamber used in the test setup. Note that Zone 1 in the figure is the standard climate range for continuous operation of the chamber and Zone 2 is standard climate range for discontinuous operation only (dew points ranging from +4 °C to -3 °C).

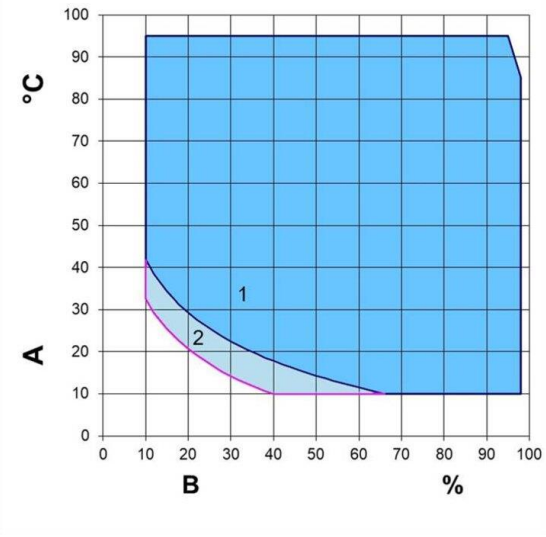

Figure 13: Humidity control diagram for WeissTechnik ClimeEco Series climate chambers

3.4. Evaluation of Test Parameters

One of the goals of the experiments was assessing the influence of air pressure on the breakdown voltage for the test object. To have a sound assessment of the inclination of the changes in the breakdown voltage, several values of possible altitudes the electric aircraft can operate at were picked, and 5 shots of negative and positive polarity high voltage tests were conducted at each of the corresponding atmospheric pressure levels.

The air pressure level for each of the altitude values were calculated using the formula

$$P(h) = 101.325 \cdot (1 - 2.25577 \cdot 10^{-5} \cdot h)^{5.25588} \qquad (4)$$

where *P(h)* is the air pressure in Pascals as a function of altitude and *h* is the altitude above sea level in meters.

The altitudes determined as test conditions and the corresponding calculated atmospheric pressure levels are given in Table 2.

Table 2: Atmospheric Pressure Levels for Various Altitudes

Altitude		Atmospheric Pressure
feet	m	mbar
0	7,620	1,013
10,000	3,048	697
15,000	4,572	572
20,000	6,096	466
25,000	7,620	376

Another goal of the experiments was assessing the influence of ambient temperature and humidity on the breakdown voltage for the test object. To obtain a large enough set of data that enables evaluation of changes in the breakdown voltage, several values of ambient temperature and relative humidity points that the electric aircraft is likely to experience were picked, and 5 shots of negative and positive polarity high voltage tests were conducted at each of the points. The tests were conducted at sea level air pressure. The temperature and relative humidity levels determined for the tests are given in Table 3.

Table 3: Test Temperatures and Relative Humidity Levels

Temperature	Relative Humidity
°C	%
-40	0
-20	0
-5	0
20	30
40	30

3.5. Test Voltage Polarity and Rate of Rise

As investigated in *Background and Theory* section, voltage polarity is known to have influence on the breakdown voltage level for insulation systems with non-homogenous electrical field distribution. As it is the case for most of the complex industrial designs, the test object being subjected to the experiments in this study had nonsymmetrical elements and was prone to the possibility of having distinct levels of breakdown voltage for positive and negative test voltage polarity. To address the possible differences in breakdown voltages, all tests were conducted for both DC polarities.

Another important parameter for assessing the breakdown voltage is rate of rise of voltage, which may cause faulty measurements or erroneous estimations due to transient phenomena when too steep and unnecessary prolongation of electrical stresses on the test object when too broad. In accordance with IEC 61180, the ramping rate of the test voltage was kept as close as possible to the recommended 5% of the final test voltage per second at the terminal stage, with the maximum absolute voltage increase rate of 650 V/s, and the test duration was limited to 60 seconds [19].

4

Results

In this chapter, the results of the thesis experiments are presented in two distinct sections: the vacuum chamber tests and the climate chamber tests. As the voltage polarity effect for the complex test object geometry and the wide coverage of test conditions range cannot be predicted, all the tests are conducted for both polarities of the direct current test voltage, namely positive and negative polarities. Figure 14 and Figure 15 show typical voltage waveform and insulation breakdown phenomena as well as the respective breakdown voltage.

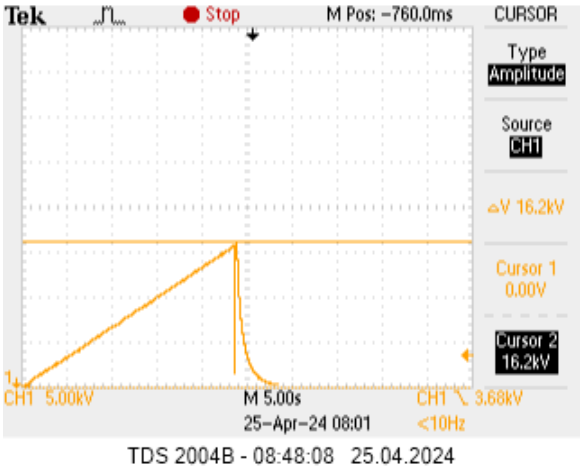

Figure 14: Typical waveform for positive polarity breakdown test

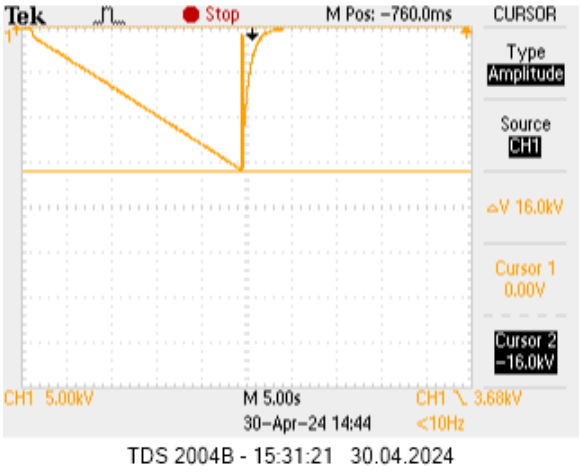

Figure 15: Typical waveform for negative polarity breakdown test

For all breakdown tests conducted in the vacuum chamber tests and the climate chamber, the breakdown occurred between the closest points of the electrodes, the fuse link plate on the applied DC potential and mounting screw of the fuse base at ground potential. See Figure 16 and Figure 17 showing the air breakdown between the electrodes of the test object and typical breakdown paths for the test object respectively.

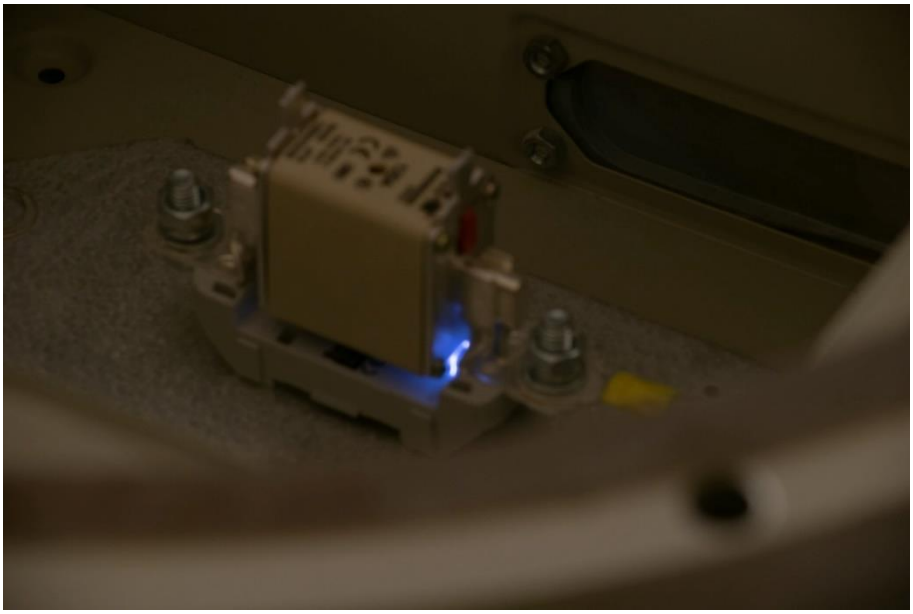

Figure 16: A photograph of air breakdown between the electrodes of the test object

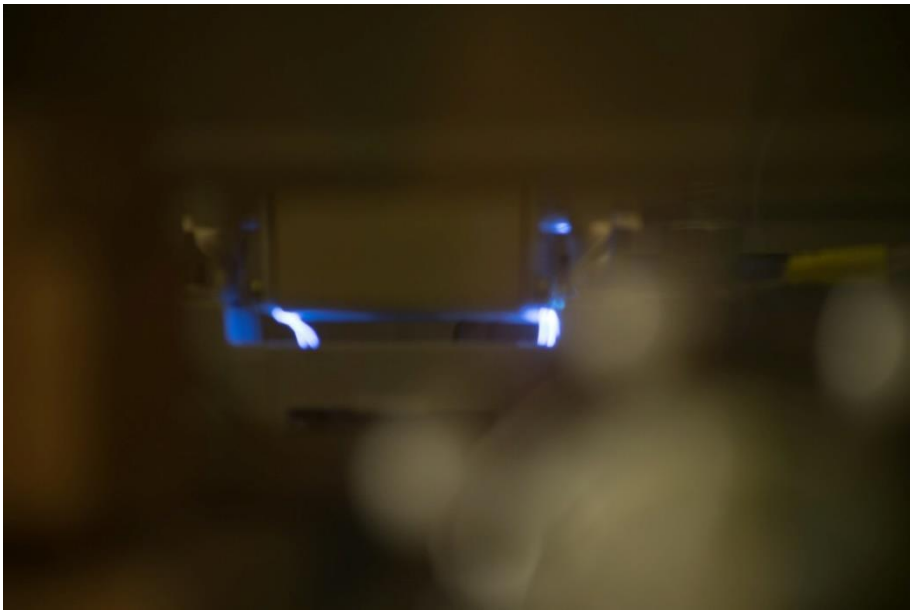

Figure 17: Typical breakdown paths for the test object

4.1. Results for the Vacuum Chamber Tests

Figure 18 shows the positive breakdown voltage measurements of the insulation system as a function of air pressure. Breakdown voltage is given in kilovolts DC (kV_{dc}) on the left y-axis and air pressure in millibars (mbar) on x-axis. The right y-axis shows the depreciation in the breakdown voltage in percentage, taking the breakdown voltage at sea-level atmospheric pressure as reference.

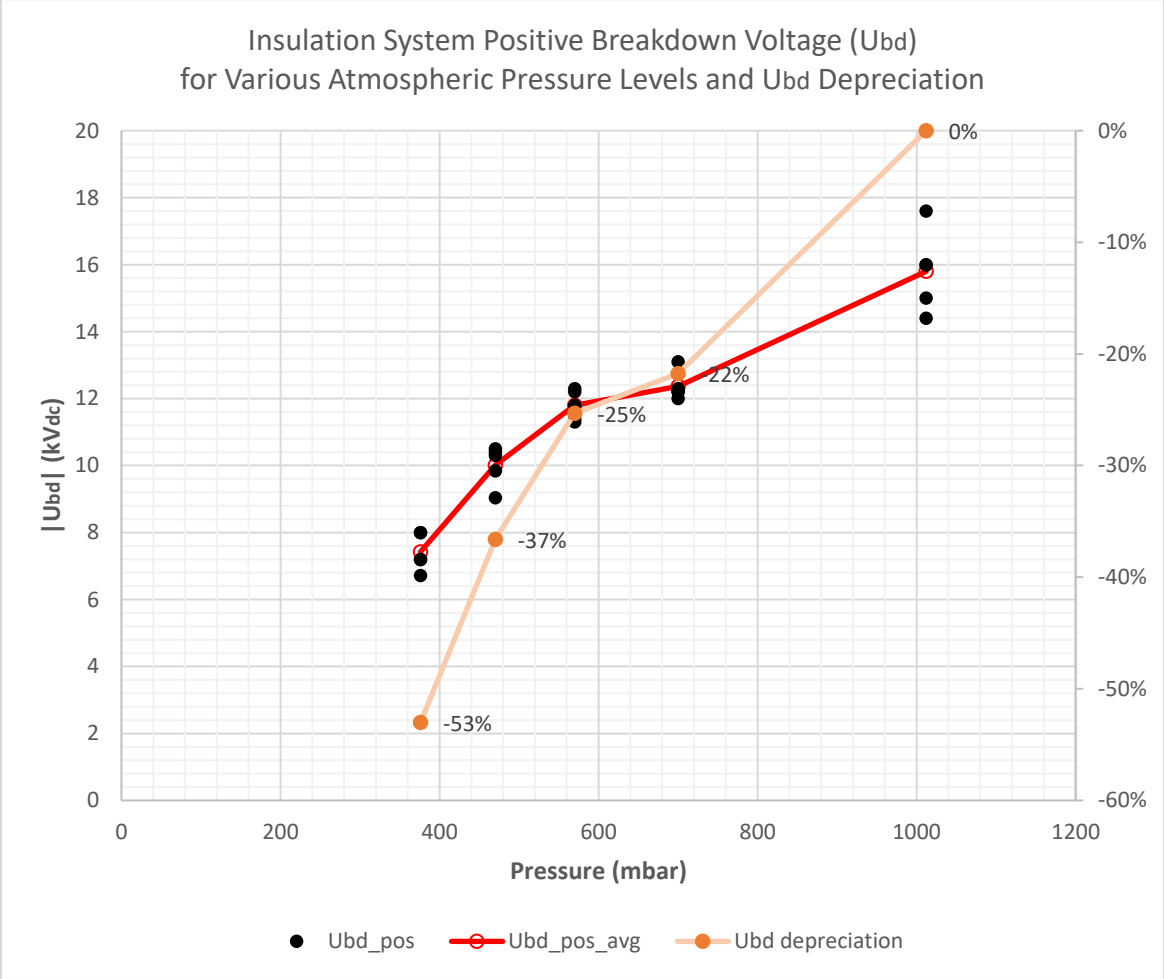

Figure 18: Insulation System Positive Breakdown Voltage (U_{bd}) for Various Atmospheric Pressure Levels and U_{bd} Depreciation

Figure 19 shows the negative breakdown voltage measurements of the insulation system as a function of air pressure. Absolute value of the breakdown voltage is given in kilovolts DC (kV_{dc}) on the left y-axis and air pressure in millibars (mbar) on x-axis. The right y-axis shows the depreciation in the breakdown voltage in percentage, taking the breakdown voltage at sea-level atmospheric pressure as reference.

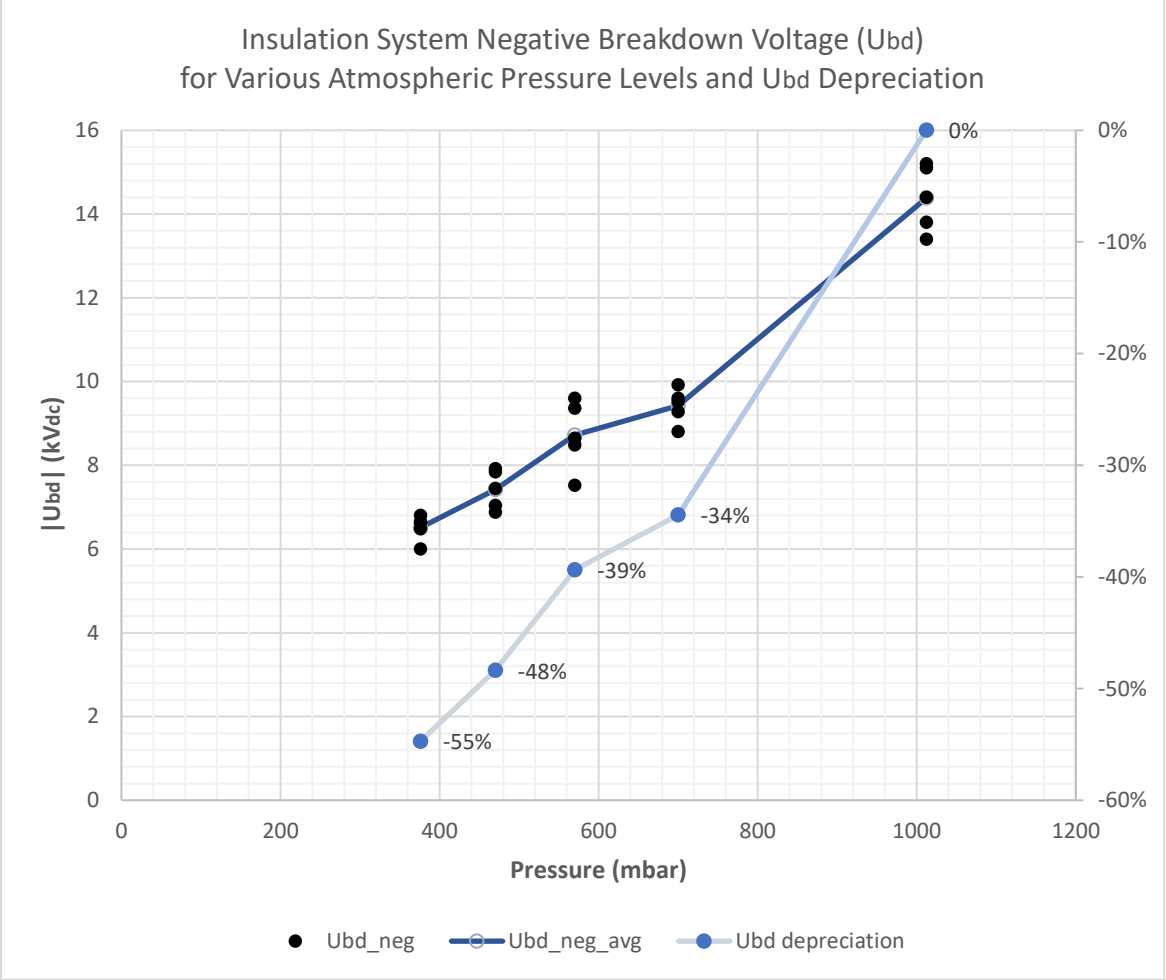

Figure 19: Insulation System Negative Breakdown Voltage (U_{bd}) for Various Atmospheric Pressure Levels and U_{bd} Depreciation

Figure 20 shows the recorded breakdown voltage levels as a function of air pressure in a voltage-polarity comparative form. Note that the breakdown voltage values are given in absolute values to allow better comparison.

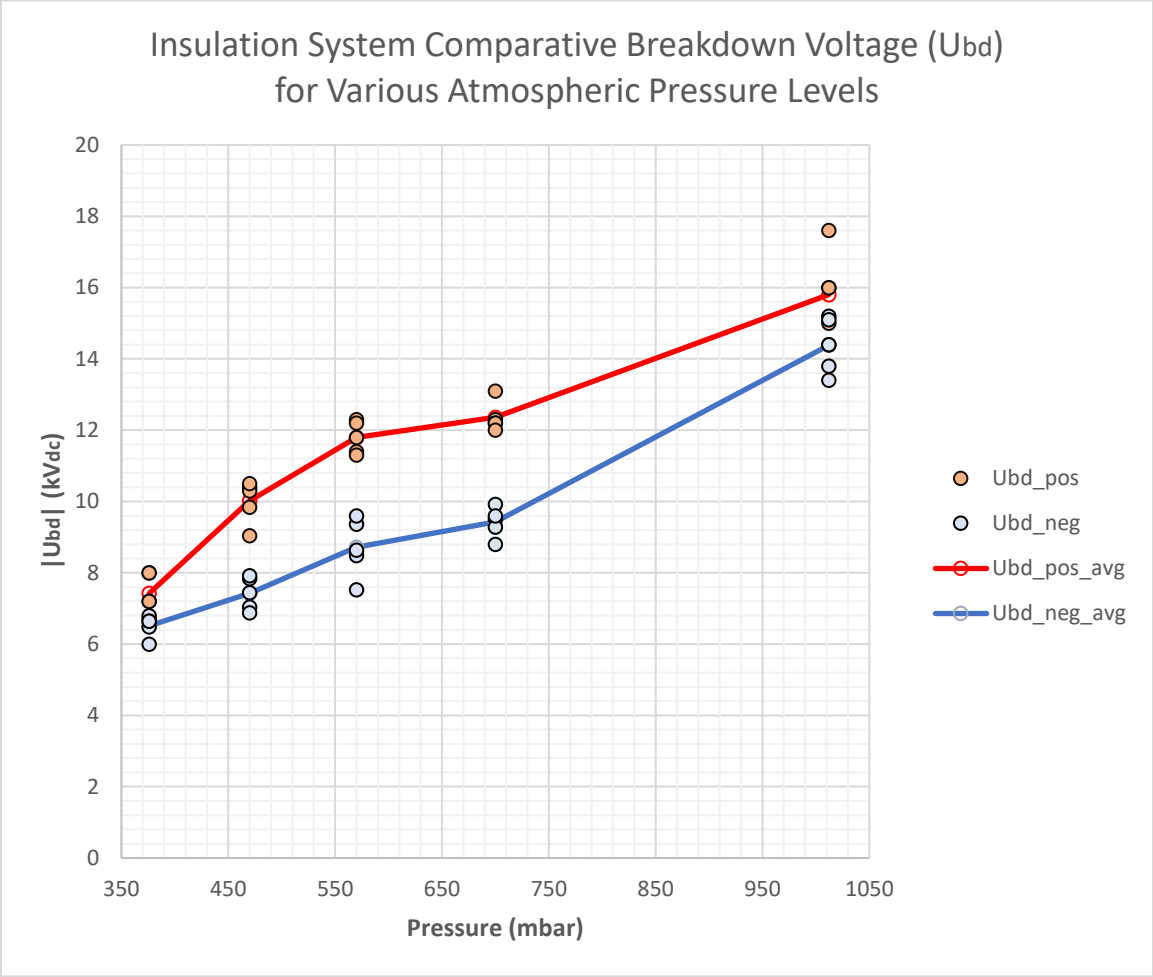

Figure 20: Insulation system comparative breakdown voltage (U_{bd}) for various atmospheric pressure levels

4.2. Results for the Climate Chamber Tests

Figure 21 shows positive breakdown voltage of the insulation system as a function of temperature and relative humidity. It must be noted that relative humidity at ambient temperature $T \leq 0$ °C is zero, as the water molecules cannot exist in gaseous form, and higher relative humidity level is achievable in controlled manner once the ambient temperature exceeds 10 °C.

Breakdown voltage is given in kilovolts (kV) on left y-axis and ambient temperature in degrees Celsius on x-axis.

The right y-axis shows the enhancement in the breakdown voltage in percentage as the temperature drops, taking the breakdown voltage at -5 °C as the reference value.

Separate trendlines were created for relative humidity (RH) levels of 0% and 30%, designated as RH0 and RH30, respectively.

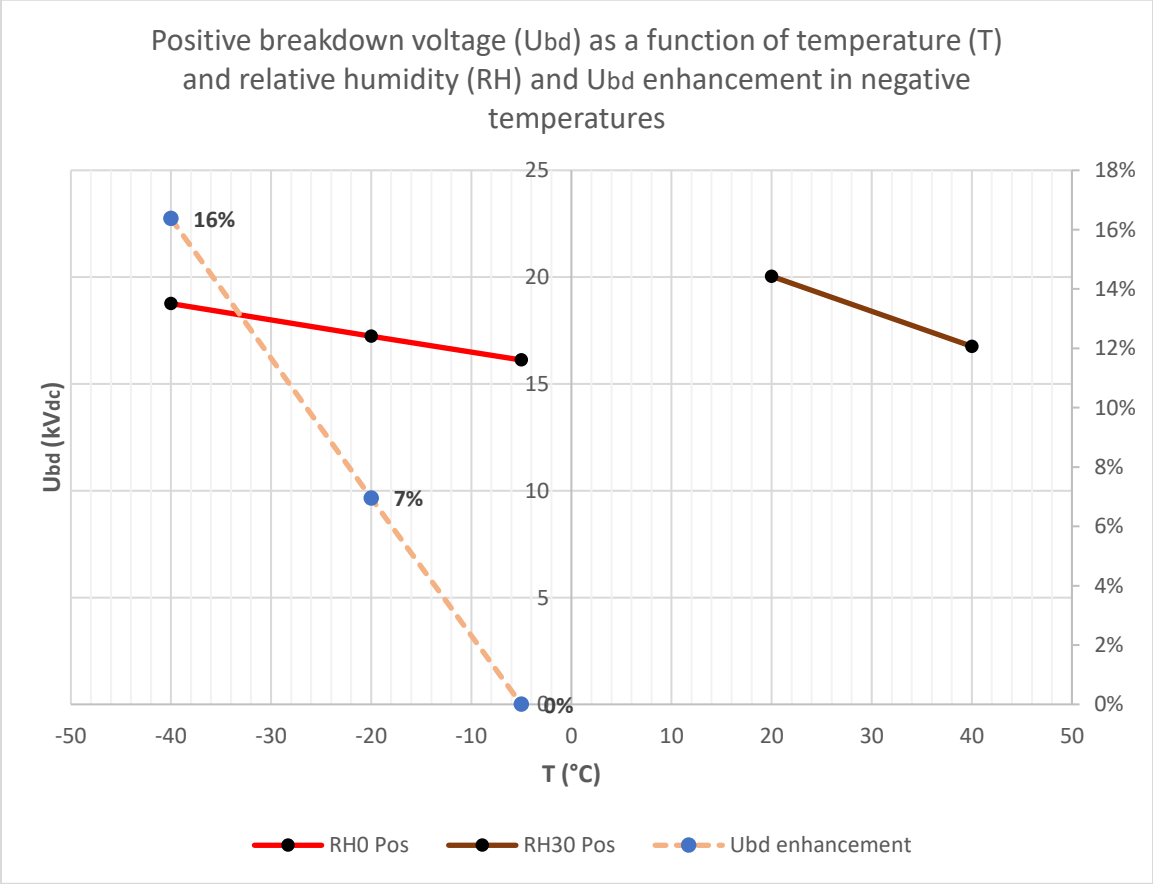

Figure 21: Positive breakdown voltage (U_{bd}) as a function of temperature (T) and relative humidity (RH) and U_{bd} enhancement in negative temperatures

Figure 22 shows negative breakdown voltage of the insulation system as a function of temperature and relative humidity. Relative humidity control limitations are the same as the positive breakdown voltage tests. Breakdown voltage is given in minus kilovolts (-kV) on left y-axis and ambient temperature in degrees Celsius on x-axis.

The right y-axis shows the enhancement in the breakdown voltage in percentage as the temperature drops, taking the breakdown voltage at -5 °C as the reference value.

Separate trendlines were created for relative humidity (RH) levels of 0% and 30%, designated as RH0 and RH30, respectively.

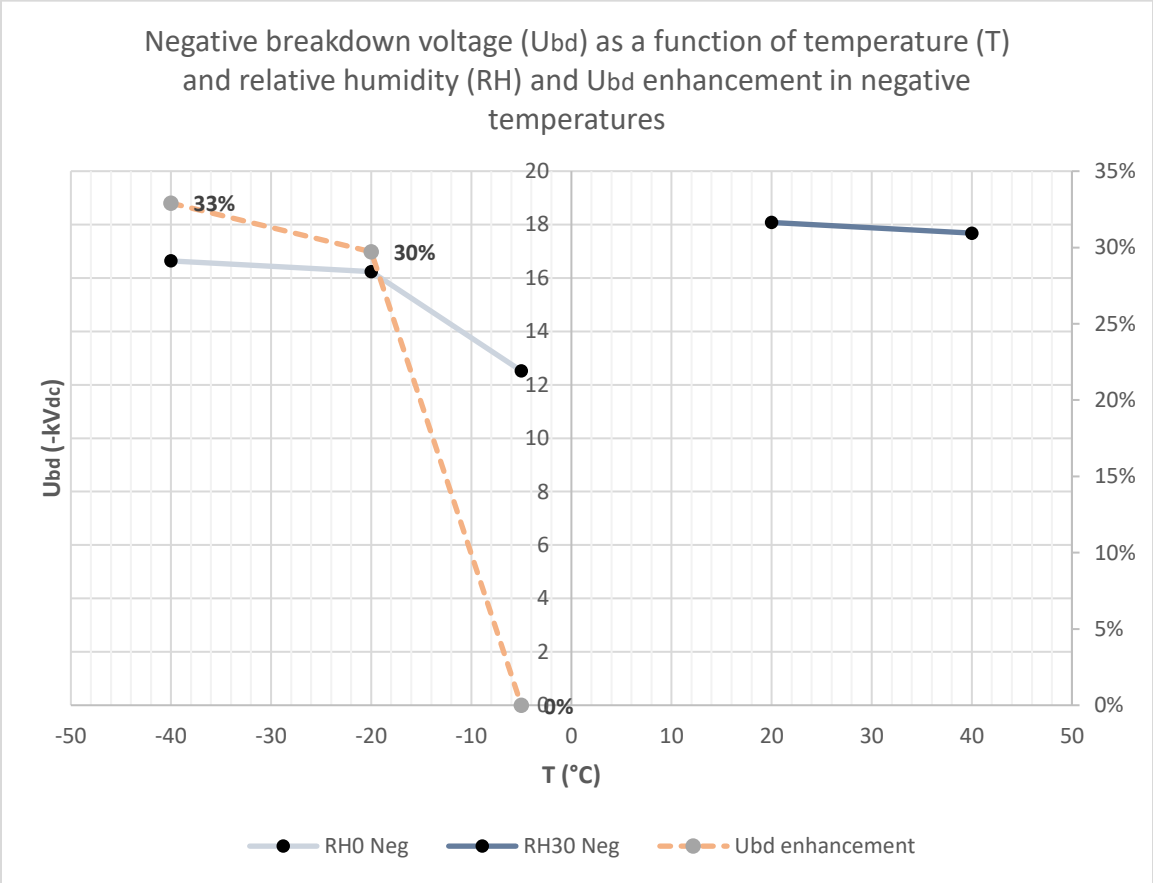

Figure 22: Negative breakdown voltage (U_{bd}) as a function of temperature (T) and relative humidity (RH) and U_{bd} enhancement in negative temperatures

Figure 23 shows the recorded breakdown voltage levels as a function of ambient temperature and relative humidity in a voltage-polarity comparative form. It must be noted that the breakdown voltage is given in absolute values for better comparison.

The breakdown voltage trendlines for ambient temperatures $T \leq 0$ °C are for 0% relative humidity conditions, while 30% RH was assumed for $T \geq 20$ °C.

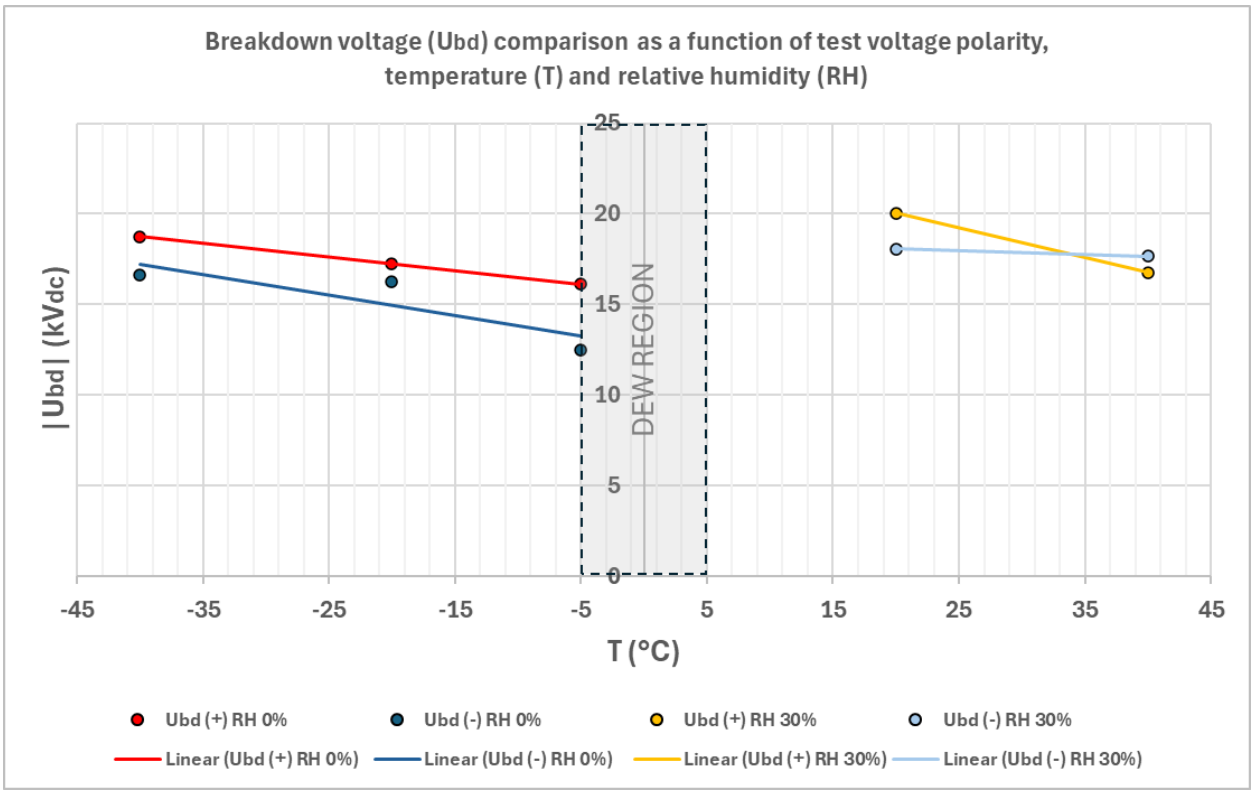

Figure 23: Breakdown voltage (U_{bd}) as a function of test voltage polarity, temperature (T) and relative humidity (RH)

5

Discussion

5.1. Discussion on the results of vacuum chamber tests

The results obtained for breakdown voltage dependence on air pressure point out a linear correlation between the air pressure and the breakdown voltage for the test specimen, as shown in Figure 24. As seen on the figure, the correlation is highly linear, which suggests that the test pressure range and the clearance between the electrodes where breakdown occurred produced a $p{\cdot}d$ range at the right side of the $U_{bd\ min}$, along the ray $\overrightarrow{CA}$, the near-linear and positive correlation zone of the Paschen curve on Figure 3.

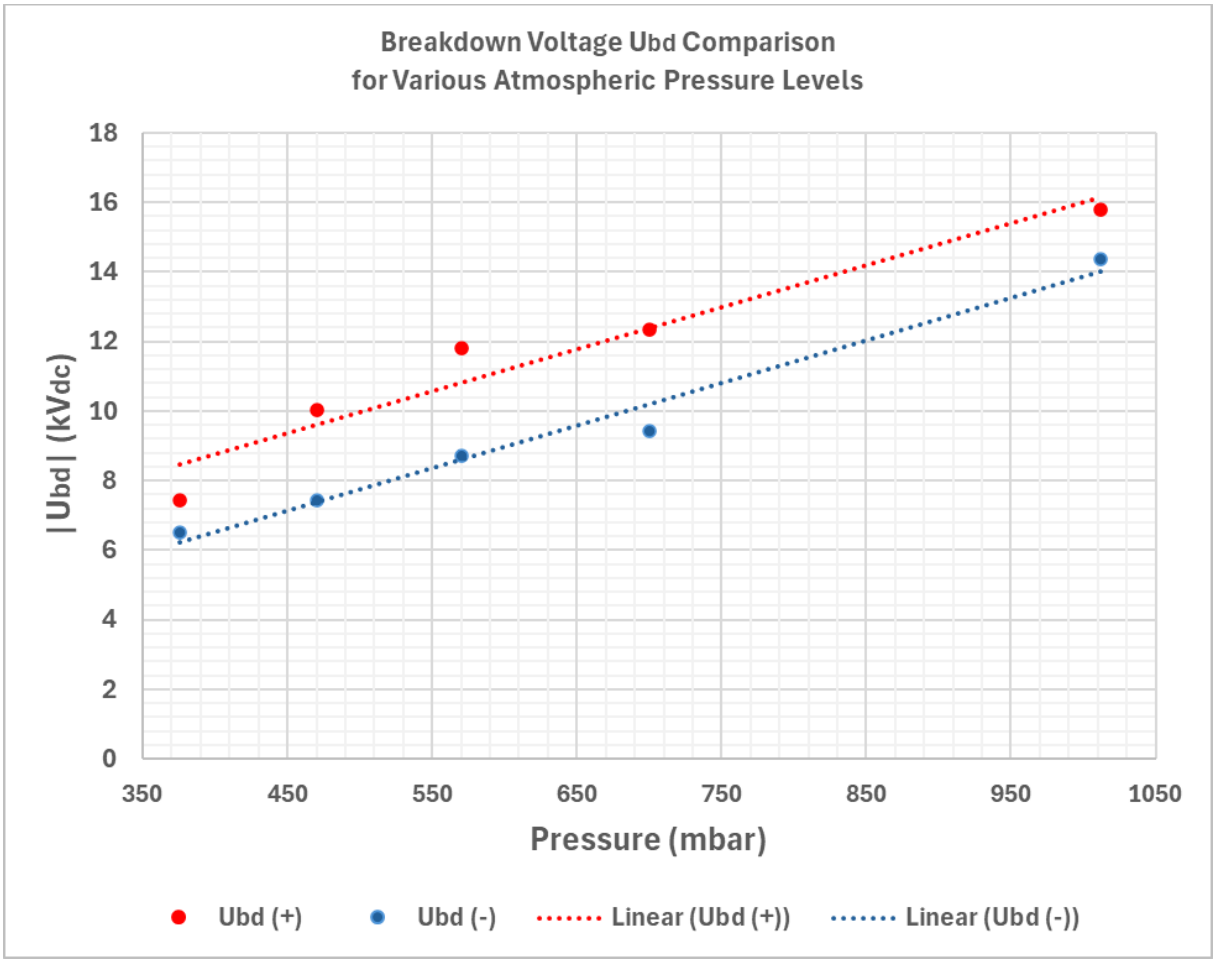

Figure 24: Breakdown voltage (U_{bd}) - atmospheric pressure level correlation chart

The slope of the linear correlation for the described range is calculated as

$$\Delta U_{bdx}/\Delta p = \frac{U_{bdx}(p_{test\ max}) - U_{bdx}(p_{test\ min})}{p_{test\ max} - p_{test\ min}} \qquad (4)$$

where *x* represents either positive (+) or negative (-) polarity indices, $\Delta U_{bdx}/\Delta p$ is change of breakdown voltage with respect to change in pressure (kV/mbar), $U_{bdx}(p)$ is the measured average breakdown voltage at a given pressure in kV, while $p_{test\ max}$ is the maximum and $p_{test\ min}$ is the minimum pressure levels applied in the test (mbar). When (4) is applied for positive (+) or negative (-) polarity tests, the rate of change values within the test range are calculated to be:

$$\frac{\Delta U_{bd+}}{\Delta p} = \frac{U_{bd+}(p_{test\ max}) - U_{bd+}(p_{test\ min})}{p_{test\ max} - p_{test\ min}} = \frac{15.80\ kV - 7.42\ kV}{1{,}012\ mbar - 376\ mbar} \approx 13.17\ V/mbar \qquad (5)$$

$$\frac{\Delta U_{bd-}}{\Delta p} = \frac{U_{bd-}(p_{test\ max}) - U_{bd-}(p_{test\ min})}{p_{test\ max} - p_{test\ min}} = \frac{14.38\ kV - 6.51\ kV}{1{,}012\ mbar - 376\ mbar} \approx 12.37\ V/mbar \qquad (6)$$

The depreciation of the voltage withstand at lower pressure levels can be attributed to the increase of mean free path for the free electrons in the air due to increased scarcity of atoms and molecules in the insulating space, providing a higher chance of ionizing collisions, thus reducing the avalanche inception voltage to relatively lower levels. The result is in line with the expectations with the phenomena Townsend mechanism describes.

5.2. Discussion on the results of climate chamber tests

The results obtained for breakdown voltage dependence on ambient temperature point out a reverse linear correlation between the ambient temperature and the breakdown voltage for the test specimen, as shown in Figure 25.

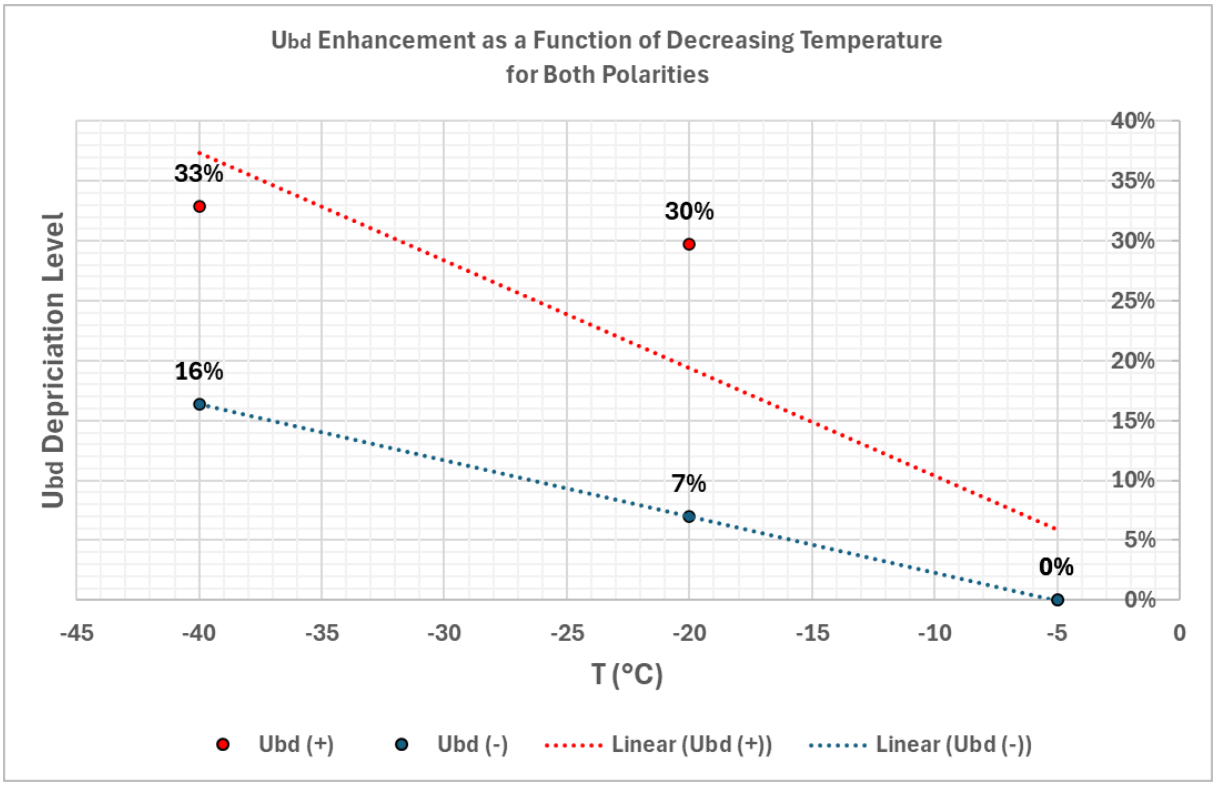

Figure 25: Change of breakdown voltage (U_{bd}) with respect to ambient temperature

The slope of the linear correlation for the described range is calculated as

$$\Delta U_{bx}/\Delta T_A = \frac{U_{bx}(T_{A\,max}) - U_{bx}(T_{A\,min})}{T_{A\,max} - T_{A\,min}} \quad (7)$$

where *x* represents either positive (+) or negative (-) polarity indices, $\Delta U_{bdx}/\Delta T_A$ is change of breakdown voltage with respect to change in ambient temperature (kV/K), $U_{bdx}(T_A)$ is the measured average breakdown voltage at a given ambient temperature in kV, while $T_{A\,max}$ is the maximum and $T_{A\,min}$ is the minimum ambient temperatures applied in the tests (K). When (7) is applied for positive (+) or negative (-) polarity tests, the rate of change values within the test range are calculated to be:

$$\frac{\Delta U_{b+}}{\Delta T_A} = \frac{U_{b+}(T_{A\,max}) - U_{b+}(T_{A\,min})}{T_{A\,max} - T_{A\,min}} = \frac{16.12\ kV - 18.76\ kV}{268\ K - 233\ K} \approx -75.43\ V/K \quad (8)$$

$$\frac{\Delta U_{b-}}{\Delta p} = \frac{U_{b-}(T_{A\,max}) - U_{b-}(T_{A\,min})}{T_{A\,max} - T_{A\,min}} = \frac{12.52\ kV - 16.64\ kV}{268\ K - 233\ K} \approx -117.71\ V/K \quad (9)$$

The depreciation of the voltage withstand at higher gas temperatures can be attributed to the fact that temperature rise increases the gas pressure, resulting in escape of atoms and molecules in a fixed volume that is not hermetic, increase of mean free path for the free electrons in the air due to increased scarcity of atoms and molecules in the insulating space, providing a higher chance of ionizing collisions, thus reducing the avalanche inception voltage to relatively lower levels. The result is in line with the expectations with the phenomena Townsend mechanism describes.

5.3. Future Work

This thesis presented the gas breakdown voltage - pressure and gas breakdown voltage – temperature and humidity relations in a segregated way. However, the combined impact of potential interactions between pressure, temperature, and humidity on the breakdown characteristics of air insulation in power distribution components of electrical aircraft is yet to be further explored.

Considering the wide range of environmental conditions that an aircraft is likely to experience, often within the same flight, with dramatic rate of changes in the parameters, another area that needs future attention is the phenomena occurring around the dew point of water and the implications on the voltage withstand of power distribution components. As seen in Figure 23, U_{bd} follows the gas density law, where the air inside the climate chamber is dry and no icing appears on the surfaces of the test object. As the temperature increases and reaches close to the dew point of water between -5 °C and 5 °C, moisture tends to condensate on metallic electrodes and across the isolation creepage paths, potentially creating ice crystals in this temperature interval in a stochastic nature, where predicting U_{bd} becomes hardly predictable.

6

Conclusion

This project ventured to investigate the influence of high-altitude ambient conditions on the insulation systems of electrical aircrafts.

From the observations made through the theoretical and experimental studies carried out during the project, it was concluded that lower air pressure creates relatively unfavorable conditions for the insulation systems due to increasing mean-free-path in the insulation gas with the decreasing concentration of air molecules, which creates better electron avalanche starting conditions.

One of the important outcomes of the project was that the decreasing ambient temperature at higher altitudes improves the insulation system performance, resulting in higher breakdown voltage, while absence of water molecules in the air below water freezing point poses a disadvantage, as it leads to breakdown mechanisms taking over at lower electric field stress levels.

Another finding of the project is that higher humidity levels increase the insulation performance by intensifying the attachment processes of electrons to intrinsically electronegative water molecules, effectively reducing the number of free electrons to start avalanches.

The studies also showed that specific measures should be considered for water dewing temperatures where water molecules in the air start to condensate over the solid insulation surface and potentially form ice crystals, with potential hazard of heavily depreciated, unstable, and unpredictable performance of the insulations systems.

Combining the observations for various ambient conditions, it is concluded that ambient conditions at altitudes up to 25,000 feet depreciate the performance of insulation systems of electrical aircrafts in a proportionally worsening manner, while the most hazardous conditions occur around the phase transition temperatures of humidity in the air with less predictable consequences in terms of breakdown voltage levels.

References

[1] IBM, "What are environmental issues?," IBM, [Online]. Available: https://www.ibm.com/topics/environmental-issues. [Accessed 09 05 2024].

[2] Earth.org, "15 Biggest Environmental Problems of 2024," [Online]. Available: https://earth.org/the-biggest-environmental-problems-of-our-lifetime/. [Accessed 09 05 2024].

[3] NOAA National Centers for Environmental Information, "2023 was the warmest year in the modern temperature record," 17 01 2024. [Online]. Available: https://www.climate.gov/news-features/featured-images/2023-was-warmest-year-modern-temperature-record. [Accessed 09 05 2024].

[4] U.S. Global Change Research Program, "2022–2031 Strategic Plan," Washington, DC, 2022.

[5] "Major climate benefits with electric aircraft," Swedish Electromobility Center, [Online]. Available: https://emobilitycentre.se/major-climate-benefits-with-electric-aircraft/. [Accessed 08 05 2024].

[6] "Reducing emissions from aviation," European Comission, [Online]. Available: https://climate.ec.europa.eu/eu-action/transport/reducing-emissions-aviation_en. [Accessed 08 05 2024].

[7] J. D'souza, "The Future of Aviation: Aircraft Electrification," Cranfield University, 06 02 2020. [Online]. Available: https://blogs.cranfield.ac.uk/aerospace/the-future-of-aviation-aircraft-electrification/. [Accessed 09 05 2024].

[8] J. Reed, "Challenges and Opportunities for Electric Aviation," Aviation Today, 30 12 2022. [Online]. Available: https://www.aviationtoday.com/2022/12/30/challenges-opportunities-electric-aviation/. [Accessed 09 05 2024].

[9] H. Huang, "Challenges in More Electric Aircraft (MEA)," IEEE, [Online]. Available: https://tec.ieee.org/newsletter/july-august-2015/challenges-in-more-electric-aircraft-mea. [Accessed 09 05 2024].

[10] Bombardier, "Aviation Operational Measures For Fuel And Emissions Reduction Workshop: Weight Management," 2006. [Online]. Available: https://www.icao.int/Meetings/EnvironmentalWorkshops/Documents/ICAO-TransportCanada-2006/Viscotchi.pdf. [Accessed 07 05 2024].

[11] A. Küchler, High Voltage Engineering, Schweinfurt, Germany: Springer-Verlag GmbH Germany, 2018.

[12] P. J. Bada, "Electric Discharge," Scripps Institution of Oceanography, La Jolla, CA, USA, [Online]. Available: https://link.springer.com/referenceworkentry/10.1007/978-3-642-11274-4_490. [Accessed 15 05 2024].

[13] "Wikipedia: Friedrich Paschen," [Online]. Available: https://en.wikipedia.org/wiki/Friedrich_Paschen. [Accessed 07 05 2024].

[14] C. Wadhwa, High Voltage Engineering, New Age International Ltd., 2007.

[15] "Wikipedia: Paschen's Law," [Online]. Available: https://en.wikipedia.org/wiki/Paschen%27s_law. [Accessed 07 05 2024].

[16] C. B.-S. 3. By Cmglee - Own work, "Phase diagram of water including high-pressure forms ice II, ice III, etc.," [Online]. Available: https://commons.wikimedia.org/w/index.php?curid=14939155. [Accessed 18 05 2024].

[17] WeissTechnik, "The new Eco range from Weisstechnik – standard Environmental Testing Chambers," WeissTechnik, [Online]. Available: https://www.weiss-technik.com/environmental-simulation/en/detailpages/climeeco. [Accessed 18 05 2024].

[18] International Electrotechnical Commission, "IEC 61180: High-voltage test techniques for low-voltage equipment - Definitions, test and procedure requirements, test equipment," International Electrotechnical Commission, 2016.

[19] E. Kuffel, W. S. Zaengl and J. Kuffel, High Voltage Engineering Fundamentals, Butterworth-Heinemann, 2000.

[20] NuclearPower.com, "Triple Point of Water," [Online]. Available: https://www.nuclear-power.com/nuclear-engineering/materials-nuclear-engineering/properties-of-water/triple-point-of-water/. [Accessed 18 05 2024].

DEPARTMENT OF ELECTRICAL ENGINEERING
CHALMERS UNIVERSITY OF TECHNOLOGY
Gothenburg, Sweden 2025
www.chalmers.se

CHALMERS
UNIVERSITY OF TECHNOLOGY